Weak pinning of interfaces

S. B. Santra, Agnés Paterson, and Stéphane Roux
Laboratoire de Physique et Mécanique des Milieux Hétérogènes,
Ecole Supérieure de Physique et Chimie Industrielles, 10 rue Vauquelin, 75231 Paris cedex 05, France
(Received 29 June 1995; revised manuscript received 27 November 1995)

We introduce a model of interface pinning on pointlike defects distributed randomly over the plane. The model is relevant for the interface between immiscible fluids in a disordered two-dimensional medium (Hele-Shaw cell) or for dislocation pinning. In the limit of small defect strength, a scaling argument is given that provides the mean curvature of the interface as a function of the defect density and strength and of the pressure. The model is also analyzed numerically in the continuum using an original transfer-matrix algorithm. The numerical results support the theoretical prediction for low defect strength. An effective surface tension at a scale much larger than that of the defect separation can be defined. The change in surface tension is shown to be proportional to $C^{1/2}\alpha^{3/2}$, where C is the defect concentration and α the dimensionless defect strength.

PACS number(s): 68.10.−m, 68.45.Gd

I. INTRODUCTION

Wetting is strongly affected by the presence of heterogeneities. The apparent surface energy is modified by the presence of defects and, moreover, hysteretic effects appear that signal the limitation of the notion of an effective (average) surface tension [1,2].

Concerning the morphology of these interfaces, some recent progress has been achieved through the description of their motion by a Langevin equation [3,4]. The most common problem that has been addressed recently is the detailed shape of the interface between immiscible fluids in a quasi-two-dimensional case. This upsurge of activity was first motivated by the disagreement between the prototypical example of interface motion in a noisy environment, i.e., the Kardar-Parisi-Zhang equation [5], and a series of experimental results [6]. This recent effort has emphasized the importance of a quenched heterogeneity versus an annealed noise [3,4].

Apart from the Langevin equation approach, some more specific models, such as the one introduced by Čieplack and Robbins [7,8], have been introduced in the past in order to model the fluid interface in idealized two-dimensional media. Although two and three dimensions exhibit serious differences, the two-dimensional case already contains part of the intrinsic difficulties and corresponds to physical cases (wetting in a confined geometry [9], dislocation pinning, etc.). The interest of these models is to avoid the introduction of simplifying assumptions that are not totally controlled (such as the representation of the interface as a single-valued function, which may lead to the question of the relevance of directedness in such models). One conclusion of Čieplack and Robbins is that one encounters two distinct regimes depending on the defect strength. A large strength gives rise to an invasion percolation model. In this case, the easiest pore is invaded at each time step. No collective motion is implemented in this model (although "bursts" or "avalanches" can be defined *a posteriori* [10]). The weak disorder case gives rise to a very different behavior where invasions are not triggered by single defects, but rather correspond to collective processes [8,11]. The weakness of this model comes from the purely geometric construction of the invasion domain and thus the absence of a real dynamics based on a description of the viscous flow. The described evolution from a given configuration results from the successive application of simple geometrical constructions.

We introduce a model in a similar spirit, whose aim is thus *not* to describe the dynamics of the real motion. We rather focus on the possible interface conformations under specific conditions. The question of whether these conformations are really accessible will not be addressed, although some major difference may arise from this constraint. Our model bears some of the features of the directed polymer problem [3] and of spiral percolation [12].

II. MODEL

For the sake of concreteness, we will discuss the construction of our model with respect to an application for a two-fluid interface in a two-dimensional medium. If we consider a Hele-Shaw cell with a constant thickness h (along the z direction) and an interface between two fluids that has a small curvature in the (x,y) plane, the two curvatures decouple and it is possible to integrate all z dependences. The Laplace law relates the pressure drop across the meniscus to the total curvature $\Delta p = \gamma(1/R_1 + 1/R_2)$, where γ is the surface energy of the interface between the two fluids and R_1 and R_2 are the two principal radius of curvature. A full integration in the z direction permits one to express the pressure drop across the interface as a function of the curvature $1/\rho$ in the (x,y) plane as

$$\Delta p = \gamma\left(a + \frac{b}{\rho}\right). \tag{1}$$

In this expression a depends on the cell thickness, as well as on the spreading coefficients S, defined as $S = \gamma_1 - \gamma_2$, the difference of surface energies, where γ_1 and γ_2 are the surface energies between the wall and fluid 1 and the wall and fluid 2, respectively. The other coefficient b is a numerical factor that also depends on the wettability of the walls. In the case of a completely wetting fluid the factor $b = \pi/4$, as established by Park and Homsy [13].

A defect in this problem can be represented as a small zone on one wall of the Hele-Shaw cell with different wettability properties. It is possible to solve exactly the deformation of the interface as it passes on the defect. However, this problem involves some subtleties, such as a kink of the interface as it crosses the defect boundary, which are not expected to play any major role in a coarse grained description. Moreover, the local distortion of the interface is very dependent on the defect shape.

This constitutes a motivation for defining an "equivalent" defect whose size is reduced to a point. Of course, in so doing, one should define properly the characteristic feature of the defect to be considered. Let ΔS be the difference of spreading coefficients of a clean surface and that of a surface with defects and d is the size of the defects. The force exerted on the defects by the interface due to the wettability of the walls is proportional to $d\Delta S$. Conversely, distorting the interface gives rise to a force proportional to the cell thickness and the two fluid surface energy $h\gamma$. When gravity is unimportant, it has been shown [14] that the strength of the defect could be well captured by a dimensionless coefficient $f = d\Delta S/h\gamma$. Keeping f constant as d goes to zero leads to the equivalent pointlike defect we were looking for.

As the defect size goes to zero, the strength f is an appropriate measure of its strength. However, we would like to introduce another quantity that is directly related to f. The maximum force that a defect can support can be uniquely characterized by the change of angle α that the interface can assume before passing across the defect or encircling it. This angle has, moreover, a simple geometric definition (see Fig. 1) and thus can easily be accessed experimentally. Some simple computation shows that this angle is uniquely a function of f and thus is fully consistent with the notion of pointlike defects. We will thus stick to this definition in the following.

It is interesting to note here that the pointlike defect is a singular limit that introduces a different feature in the problem. Indeed, when the size of the defect is greater than zero, the interface shape is a well defined problem. Specifying the starting point and tangent, then the interface shape is uniquely determined. When the defect size goes to zero, all configurations of interfaces that go through the defect cannot be distinguished. Thus an interface that reaches the defect can either leave the defect undisturbed, as if it was just tangent to the defect, or it can be bent on the defect by any angle in the interval $[0, \alpha]$ if α denotes the strength of the defect. Thus we have lost the uniqueness of the solution. This is an essential feature also related to the appearance of hysteretic effects on a surface supporting pinning sites.

Let us now introduce our model. The surface is characterized by a random Poisson distribution of pointlike defects. The area concentration is C and the defects' strength is equal to α. We introduce a pressure ΔP such that the radius of curvature of the interface on a clean surface is R. We deal with a static problem so that the pressure is uniform in the fluid. Thus a typical interface configuration consists of arcs of circle of radius R between defects, as shown in Fig. 2. On a defect the interface can bend and get an angular discontinuity θ such that $\theta \in [0, \alpha]$. The latter rule implies that a large number of interfaces with the same starting point and tangent can be found.

These interfaces are called "admissible" if they obey the above rules. The complete enumeration of these admissible conformations is generally impossible. As we mentioned above, any physical interface *has to be* admissible. However, incorporating a faithful dynamics may select as accessible only a subset of all admissible interfaces. Our goal is here to try to explore some properties of admissible interface geometries, leading to bounds on accessible interfaces. We underline that no statement can be made on the possible accessibility of a particular interface conformation from an initial state. Although it is quite possible that under a given dynamics this accessibility makes the observed interfaces different from the one we characterize here, such a difference is, however, expected to vanish for small defect strength.

To characterize our problem, we compute the upper envelope of all admissible interfaces. We will in the following compute the large scale curvature of this envelope, which is definitely an upper bound on the curvature of all admissible and thus accessible interfaces.

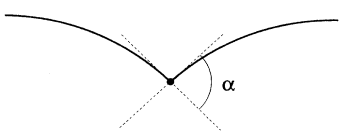

FIG. 1. The defect, shown here as a black dot, is characterized by the maximum angular discontinuity α the interface can assume on the defect. Keeping α constant, we consider here defects whose physical size tends to zero.

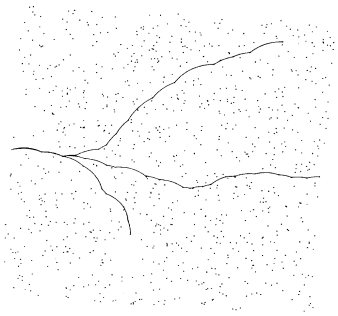

FIG. 2. Example of interfaces going through defects for a fixed defect strength α. Different interfaces correspond to different R, the radius of curvature on the clean surface.

III. NUMERICAL SIMULATIONS

The algorithm we have chosen in order to compute the envelope of all interfaces is a transfer-matrix method. We first distribute points (defects) randomly in a rectangle of size $R \times 1$, with the prescribed concentration C. In order to initialize the system, we consider that all sites in the lower half of the rectangle can be reached by an interface with an incident angle on the defect equal to 0. These sites are called "active." Then a new rectangle is considered to the right of the preceding one, as shown in Fig. 3. Starting from any active site, we construct all possible arcs that connect to another site such that the angular discontinuity at the starting defect is in the admissible interval $[0, \alpha]$. The sites that can be reached are then called active and the angle of the interface reaching the defect is recorded. In the spirit of considering an upper bound on the curvature, only the largest incident angle is kept. Once all possible active sites have been considered, we can forget about the first rectangle and keep only the list of the active sites (together with their respective incidence angle) in the last rectangle. Then a new rectangle is generated and the same procedure is applied again as many times as needed. In each rectangle, the topmost active site is recorded.

The mean (large scale) shape of interfaces is circular, as will be demonstrated below. Thus, in order to follow the interface for a large distance, we have added some flexibility in the relative position and orientation of each rectangle. More precisely, we first translate the rectangle vertically so that its mean height is equal to that of the topmost site of the preceding rectangle. Then the rectangle is rotated so that the mean incident angle becomes horizontal. However, we limit the rotations to a maximum value such that the new rectangle never overlaps the second neighboring rectangle on the left. When the rotation is not zero, we add points only in the domain that is not already covered by the preceding rectangle. The number of points is computed so that the same concentration is obeyed.

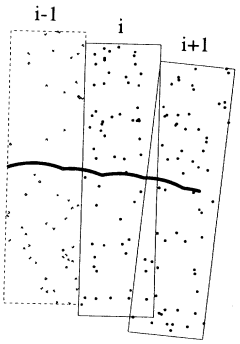

FIG. 3. Schematic plot of the transfer-matrix algorithm used. We proceed in series by considering a series of rectangles such as the three shown in the figure. We compute for each point in the rectangle $(i+1)$ if it can be reached from an accessible site of the previous rectangle (i). In this case, it becomes accessible. Only the accessibility in the previous rectangle is needed and thus the status of sites in rectangle $(i-1)$ can be forgotten. In order to follow the envelope of all interfaces, we allow the rectangles to be translated or rotated with respect to the previous one. The overlap of rectangles is taken care of.

The strip that is generated this way can achieve almost any conformation and thus we can follow the envelope even if the mean curvature is not zero. Figure 4 shows such an example. In order to get good statistics, we deliberately ignored the eventual overlap of the strip with its past, provided the overlap takes place at distances such that more than two rectangles are involved. Locally, in two consecutive rectangles, all interfaces fulfill self-avoidance. In the case of a large scale crossing of the interface with itself, then the total envelope geometry is not physically meaningful, but it provides a natural way to accumulate a long series of data and thus get an accurate estimate of the curvature. Moreover, pieces of it that are not too long are physically acceptable conformations. This trick of forgetting large scale self-avoidance of the strip can be seen as a way to perform an ensemble average with the least possible size effect due to the initialization of the active sites in the first rectangle.

The parameters of the model are the defect concentration C, defect strength α, and radius of curvature on the clean surface R. What is measured is the effective large scale radius of curvature ρ of the envelope. Using nondimensionalization, it is possible to get rid of one parameter R. The dimensionless concentration and radii are

$$\begin{aligned} C^* &= CR^2, \\ R^* &= 1, \\ \rho^* &= \rho/R. \end{aligned} \tag{2}$$

The strength α is already dimensionless.

Of particular interest is the pressure — or, equivalently, R in our model — such that the macroscopic curvature is equal to zero, i.e., $\rho = \infty$. In the case of a radial injection of a liquid from a point, this pressure is

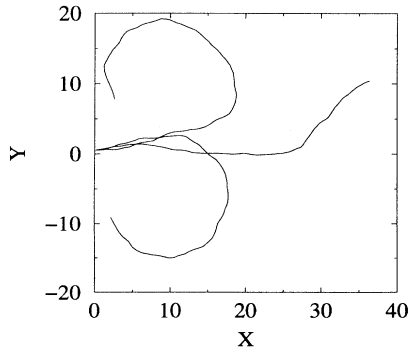

FIG. 4. Example of the envelopes computed for a fixed defect strength $\alpha = 0.22$ (12.6°). Different curves correspond to different values of C^*, the dimensionless concentration of the defects.

sufficient for the fluid to go to infinity. We will report below some analytical and numerical results concerning this breakthrough pressure. Before giving the numerical results obtained using the previously described algorithm, we will introduce an analytical approach in the limit of a weak pinning and discuss the analogy of this problem with other related statistical models.

IV. WEAK PINNING LIMIT

Let us consider the limit of weak defects that appear amenable to a scaling argument. "Weak defects" means that the maximum allowed change of angle on a defect α is small compared to unity. Since we are interested in the pressure range where the large scale curvature of the interface is close to zero (straight interface) the local curvature of the interface on a clean surface will be large. Therefore, in this limit we will substitute the circular arcs between two defects by straight segments. We will, however, reintroduce the true curvature in order to estimate the total curvature of the interface.

We consider a medium of size L and interfaces that start at a prescribed point A_0 with an orientation along the x axis. There is a large number of admissible interfaces, where angular discontinuities at each defect are less than α. We focus on the interface that has the smallest average curvature at a large distance from the starting point.

Let us consider a given interface. It consists of a set of defects (A_i) connected by arcs of radius R between each consecutive pair of defects (A_i, A_{i+1}). Let us denote by $\theta(x)$ the orientation of the tangent to the interface. Between two defects, we have $d\theta(x)/ds = -1/R$, where s is the curvilinear abscissa along the arc and thus $dx/ds = \cos(\theta)$. Let us call $d_{i,i+1} = \|A_iA_{i+1}\|$ the cord length. The change of angle along the arc is exactly $\delta_{i,i+1} = -2\arcsin(d_{i,i+1}/2R)$. Provided that we consider weak defects, we will have $d \ll R$, so that we can use the approximation

$$\delta_{i,i+1} \approx \frac{-d_{i,i+1}}{R}. \tag{3}$$

The important feature here is the fact that δ is simply proportional to the distance d between defects.

In addition to the continuous rotation of the tangent along the arcs, we also have to consider the local jumps in orientation on defects. On a defect A_i, θ is discontinuous and we have $[\![\theta]\!] = \delta_i \leq \alpha$ where $[\![\,]\!]$ denotes the discontinuity.

If A_n denotes the end point at a distance L from the starting point, the total change of angle along the interface is thus

$$\Delta = \sum_i \delta_i + \sum_i \delta_{i,i+1}. \tag{4}$$

Using Eq. (4), we see that the expression of Δ can be approximately mapped onto a directed polymer problem in random media at zero temperature [3]. In this mapping, the interface geometry would correspond to a polymer configuration. Considering the interaction energy density to be $1/R$ per unit length for the clean surface and being limited to a minimum value of $-\alpha$ on defects, the clockwise rotation of the interface $-\Delta$ would be the total energy of the polymer. The interface with the largest curvature in these conditions corresponds to the conformation of the polymer with the minimum energy, namely, the conformation obtained at zero temperature.

The mapping is only approximate because the energy gain on defects is not intrinsically determined, but rather depends on the neighboring defects. Moreover, the model contains a number of specific features that may be worth investigating in more detail before jumping to the conclusion that this model is in the same universality class as directed polymers.

One essential feature is that the model is defined in the continuum. This may appear as a detail that should not affect the universality class of the model, but some care should be taken. Indeed, since the distance between defects can be arbitrarily small, the local "curvature," estimated between two defects as the change of orientation divided by the length of the connection, is unbounded. A quantitative analysis of the curvature distribution in the Appendix reveals that the cumulative probability that the curvature exceeds x scales as x^{-2}. One should note, however, that the distance between defects has to be small in this case, so that over a fixed distance, these large local curvatures may be significantly reduced. However, it cannot be excluded that the coarse-grained description of the medium has to include a power-law distribution of large local energies. Furthermore, it is known from a pioneering work of Zhang [15] that such a wide distribution of energies can induce a breakdown of universality.

Also we would like to mention that the interface generated in the model is very closely related to the spiral percolation hull [12]. The constraint of chirality introduced in this model appears here naturally. Instead of generating the percolation cluster and then determining the hull of the cluster, one could generate the spiral path on the boundary of the cluster directly. Depending on the concentration of the system, the global curvature of these spiral paths will be different, as in the case of the interfaces in this model.

V. SCALING ARGUMENT

In order to gain some insight into the dependence of the overall behavior with the model parameters, we first develop a simple argument based on typical values. The first difficulty to face is the fact that the model is defined in the continuum. We introduce an additional (artificial) constraint on paths. For a path that reaches a defect A, we will consider continuation of this path in a cone defined by the angular interval $[\alpha', \alpha]$. The mean distance δx of the closest point in this cone to A is such that $\frac{(\alpha-\alpha')}{2\pi}\pi\delta x^2 C = 1$ or

$$\delta x = \sqrt{\frac{2}{(\alpha-\alpha')C}}. \tag{5}$$

The mean change of orientation of the path over the last one is $(\alpha + \alpha')/2$ on the defect, plus a rotation $-\delta x/R$ due to the curvature of the arc between A and the next defect. The mean curvature $1/\rho$ is thus

$$1/\rho = (\alpha + \alpha')/2\delta x - 1/R. \quad (6)$$

When α' is chosen to be close to α, the gain on the defect is close to its maximum, but δx is large so that $1/\rho$ approaches $-1/R$. On the contrary, for a small α', δx is small but the gain on the defect is small. There is an optimum intermediate value that can be determined by differentiating Eq. (6) with respect to α'. This optimum value is $\alpha' = \alpha/3$. Since the value of α' is arbitrary, we determine α' so as to maximize ρ. This leads to the expression

$$1/\rho = \frac{2}{3\sqrt{3}}\,\alpha^{3/2}C^{1/2} - 1/R. \quad (7)$$

Multiplying this last equation by R, we get the dimensionless equivalent

$$1/\rho^* = \frac{2}{3\sqrt{3}}\,(\alpha^3 C^*)^{1/2} - 1. \quad (8)$$

When the pressure is such that the macroscopic curvature vanishes $1/\rho^* = 0$, this last equation can be rewritten as

$$C^* \propto \alpha^{-3}. \quad (9)$$

From this expression we arrive at the conclusion that the curvature is simply corrected from that of a clean surface by a constant term that depends on the density of defects and on their strength. From the two-dimensional results recalled in the Introduction, we see that the expression of the line tension in the plane is not modified; however, the constant additional term that depends on the aperture of the Hele-Shaw cell is changed. This result is expected in the sense that the line tension is determined by the area of fluid-air interface, which is not affected by the presence of the defects on the walls. Moreover, the constant term in the expression of the capillary pressure does depend on the spreading coefficient of the fluid on the wall and the latter is naturally modified by the presence of defects. Therefore, the key result is that the Laplace law remains functionally valid, i.e., not affected by the presence of defects, whereas the surface energy of the wall is changed to first order by a term proportional to the square root of the concentration of defects times the cube of their strength.

VI. NUMERICAL RESULTS

The numerical simulations have been performed for different values of the defect strengths α in two dimensions. The defect strength α changes from 0.18 (10.31°) to 0.30 (17.18°). In each case the total length s of the strips is considered up to 500 and the concentration C is 1000 points (defects) per unit area. The total angle of rotation $\beta(s)$ has been determined as a function of the total length s. In Fig. 5 we have plotted $\beta(s)$ versus s for a particular value of α and R. To avoid the initialization effect on the interface we have ignored the data points up to $s = 100$ at the beginning. We see in this figure that the angle β increases linearly with the curvilinear abscissa. This implies that the shape of the envelope is circular on average. The slope of $\beta(s)$ computed from a linear regression (least-squares fit) gives the radius of curvature ρ.

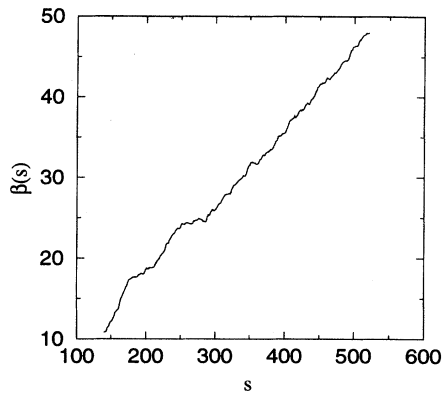

FIG. 5. Plot of the total angle of rotation $\beta(s)$ against the total arc length s for a particular value of the defect strength α and the radius of curvature R.

The macroscopic curvature has been estimated for a fixed defect strength α for different values of the pressure difference ΔP, i.e., the radius of curvature R on the clean surface. It should be mentioned that the fluctuations increase as one approaches a flat interface $1/\rho = 0$. The curvature $1/\rho$ and radius R are transformed in dimensionless quantities $1/\rho^*$ and C^* using Eq. (2). Figure 6 shows a typical evolution of $1/\rho^*$ as a function of C^*. We observe a regular evolution of the curvature, with no particular singular behavior close to zero curvature.

From these data, we can compute, for any prescribed defect strength, the concentration for which the curvature vanishes, i.e., the pressure to exert so that the invading fluid can escape to an infinite distance in a cell with a radial injection. This estimate of $C^*(1/\rho^* = 0)$,

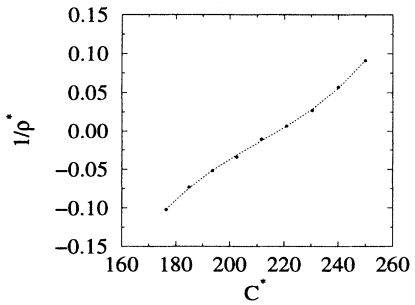

FIG. 6. Evolution of the macroscopic curvature $1/\rho^*$ as a function of the dimensionless concentration C^* for a fixed defect strength $\alpha = 0.23$ (13.27°).

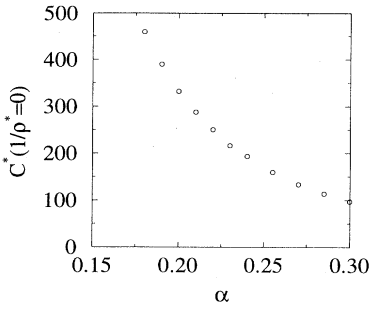

FIG. 7. Dimensionless concentration C^* for which the macroscopic curvature vanishes $(1/\rho^* = 0)$ as a function of defect strength α.

obtained by Newton's method, is shown in Fig. 7 as a function of the defect strength α.

In Sec. III, we developed a theoretical scaling argument that gives a simple scaling behavior of $C^*(1/\rho^* = 0)$ as α^{-3}. This prediction is tested in Fig. 8. We observe excellent agreement with the theoretical prediction over the entire range of α^{-3}.

There are some difficulties in obtaining the estimate of curvature for very small and very large defect strengths. In the case of a large defect strength the rotation of the strips are restricted by the maximum angle of rotation. In the case of smaller defect strengths one has to consider larger values of R and hence wider rectangles at each step of the transfer matrix; this implies more defects and finally a prohibitive increase in computer time.

Finally, we also considered the geometry of the envelope. The analogy with the directed polymer problem suggests the study of the eventual self-affinity of the interface. We analyzed the evolution of the *angle* versus the total chord length for the envelope. We computed the power spectrum of this function, taking care of the nonuniform distribution of sampling points with an adapted Fourier transform algorithm. We also got rid of the first transient part of the function and, finally, we removed the end-to-end linear variation so as to avoid introducing a spurious discontinuity in the signal. The average of the power spectrum is shown on a log-log scale in Fig. 9. A power law with a slope equal to -2 fits the

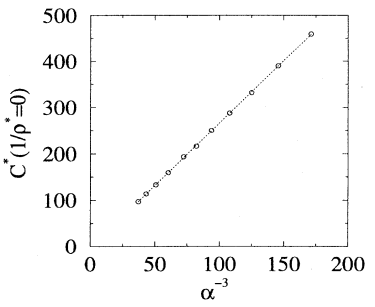

FIG. 8. Plot of C^* versus α^{-3}. The theoretical prediction $C^* \propto \alpha^{-3}$ is shown as a dotted line.

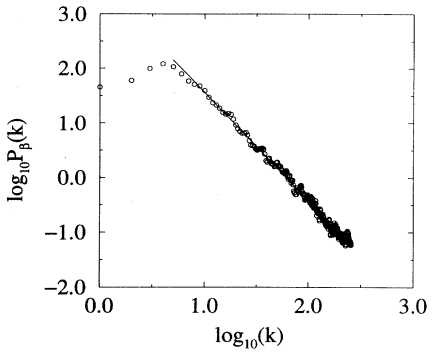

FIG. 9. Power spectrum of the slope of the interface as a function of the envelope length. A power law with an exponent -2 is shown on top of the data as a straight line.

data very well, revealing a Hurst exponent of 1/2. Therefore the derivative of the envelope behaves as a random walk, just as if the local change in angles on defects were uncorrelated. As a consequence, the envelope geometry can be compared to the *integral of a random walk* with a roughness exponent 3/2 (although some method of estimating this exponent, such as the study of the standard deviation of the height over a window of varying size, would give 1, as discussed in Ref. [16]). Therefore this conclusion violently contradicts the result that may have been anticipated by the directed polymer analogy. In the latter case the Hurst exponent of the interface would have been equal to 2/3, so that the power spectrum of its slope would have had a slope of $-1/3$, very different from the observed -2.

VII. DISCUSSION

There is abundant experimental literature on the wetting properties of heterogeneous surfaces (see, e.g., Ref. [17]). However, in most cases, these data concern three-dimensional geometries that cannot be transposed to the case of a confined fluid in two dimensions because of the nonlocal expression of the contact line energy that arises from integrating the surface deformation away from the contact line. Morever, the surface heterogeneities are seldomly characterized in a quantitative fashion. Thus a meaningful comparison with our result cannot be drawn.

Some recent experimental work has been carried out in a Hele-Shaw cell with controlled heterogeneities [18,14]. The pressure, however, could not be measured in this set-up and thus a quantitative comparison with our prediction is impossible. It would be of great interest to quantify these measurements and estimate the change in surface energy due to the presence of a defect.

The most severe weakness of our model is the absence of a proper description of the dynamics of the interface. We simply consider configurations of the interface and among these we postulate that the one with the largest curvature is significant. However, in our model, as well

as in a number of others, there is a very large number of possible configurations that fulfill the prescribed boundary conditions. Therefore, the equilibrium configuration reached at some stage assuming a quasistatic external forcing cannot be simply determined by the geometrical constraints on the interface. The full dynamics is necessary to find the correct equilibrium state. Depending on the relative weights of viscous friction, inertia, and interaction energy terms, different configurations can be reached. More importantly, not only the precise conformations are susceptible to differ, but also the statistical features may be drastically altered.

It is worth emphasizing that the same weakness affect most models that intrinsically ignore the true dynamics. Examples include *sandpile models* [19], which in most cases do exhibit self-organized criticality, but are in conflict with most experimental observations of real sandpiles [20]. Hysteretic effects, which have been often invoked to explain this discrepancy, are essentially due to inertia effects of falling sand grains. *Quasistatic invasion* of porous media by a nonwetting fluid has been often claimed to be described by invasion percolation [21]. However, the proper dynamics of the invasion is at variance with predictions of this model. A proper description of additional dynamics, such as that proposed by Måløy *et al.* [22], dramatically alters the statistics of "avalanches" in the pressure signal, which is no longer a simple power-law distribution. The frictional motion of spring-block systems (Burridge-Knoppof model), which has been claimed also to be critical generically [23], also escapes from criticality when the dynamics is carefully integrated numerically [24]. Systems for which the model could eventually be relevant must (i) have negligible inertia and (ii) be overdamped.

It is worth emphasizing the deep analogy between the problem considered in the present study and the pinning of dislocations by impurities in metals. The latter subject has received considerable attention in the past [25]. In particular the collective role of defect arrays has been highlighted through pioneering works by Friedel [26] and Mott and Nabarro [27] to cite only seminal contributions to the subject. Friedel has given an argument based on the work needed to go across a defect, which leads to an expression of the yield stress σ_y scaling as

$$\sigma_y \propto \alpha^{3/2} c^{1/2}, \tag{10}$$

where α and c have the same meaning as introduced earlier. It is to be noted that the result recovers precisely the scaling dependence of the line tension in our analysis, although the route to the result is rather different. It has been argued that this result holds only for dilute and strong defects, whereas, for concentrated and weak defects, Mott and Nabarro have proposed an alternative approach, which leads to a different scaling

$$\sigma_y \propto \alpha^{4/3} c^{2/3}. \tag{11}$$

The latter prediction is based on a "random-walk" type of geometry of the dislocation with straight connections between pinning sites. Although the two predictions are different, it is difficult to distinguish between them considering the experimental data and the small range of variation of α in most cases.

The surprising feature in the comparison between the classical approaches to dislocation pinning and the wetting interface problem developed here is the close correspondence of our result with Friedel's scaling law, in spite of the fact that it should apply only for strong defects. Our numerical results, together with the theoretical analysis provided above, suggest that the limitation generally accepted for Friedel's analysis might not be relevant. We note that Mott and Nabarro's result is not observed in our numerical simulation, although we considered weak defects for which it should hold. It should finally be noted that all analytical approaches to the problem ignore correlations in the spatial distribution of pinning sites as well as the "dynamics" of the problem — resorting to static equilibrium considerations — and thus they rely on some assumptions concerning the interface or dislocation line geometry, which has to be confirmed, finally, by either experiments or numerical simulations.

VIII. CONCLUSION

We have introduced a geometrical model of interface pinning defined in the continuum with a Poisson distribution of pinning sites or defects. We have introduced a maximum limit for all admissible interfaces, as "envelopes." The latter provide a natural way to get an accurate estimate of the maximum curvature of the interface and give access to a numerical study through an efficient and original transfer matrix algorithm. We have observed a regular evolution of the curvature of the interface envelope with the concentration for a fixed defect strength without any particular singular behavior at zero curvature. It is also found in our model that the Laplace law is obeyed at the macroscopic level, which allows us to define an effective surface energy on a substrate with random defects. This macroscopic surface energy is modified from that of the clean surface by an additional term that depends nonlinearly on the defect concentration and on the defect strength. This property, derived by a simple scaling approach, is confirmed by the results of the numerical simulations.

ACKNOWLEDGMENTS

The model studied in this paper partly resulted from discussions with A. Hansen, whom we thank warmly. We also acknowledge useful discussions with E. Charlaix, M. Fermigier, H. J. Herrmann, L. Limat, and M. O. Robbins. S. B. S. acknowledges the financial support from the French Ministry of Foreign Affairs. We thank the CNRS Groupement de Recherche "Physique des Milieux Hétérogènes Complexes" for partial support.

APPENDIX: CURVATURE DISTRIBUTION

Two defects that are very close, with a particular orientation, can give rise to a large curvature locally. The

probability distribution of these curvature has a power-law tail, which can be estimated as follows.

Let us consider a defect located at the origin and an interface that arrives on this first defect parallel to the x axis. After the defect the interface is an arc of a circle, which can be written

$$y = ax - x^2/2R, \tag{A1}$$

where a is the tangent orientation right after the defect, and thus fulfills $0 < a < \alpha$.

The effective curvature σ is defined as the change of angle divided by the distance. For weak defects $\alpha \ll 1$, the curvature can be written

$$\sigma = a/x - 1/R. \tag{A2}$$

The probability that the curvature exceeds a value s is thus equal to the probability that a defect is located in the domain

$$\begin{aligned} y &\leq \alpha x - x^2/2R, \\ y &\geq (s + 1/2R)x^2. \end{aligned} \tag{A3}$$

Since we deal with a Poisson distribution, this probability is

$$\begin{aligned} P(\sigma > s) &= \int_0^{\alpha/(s+1/R)} \alpha x - (1/R + s)x^2 C dx \\ &= (1/6)C\frac{\alpha^3}{(s + 1/R)^2}. \end{aligned} \tag{A4}$$

Thus the local curvature distribution can achieve large values locally. Due to the behavior of $P(s)$ at infinity $P(s) \sim s^{-2}$, the second moment of the curvature distribution diverges. Therefore, this distribution has an infinite variance. This feature may induce locally very strong pinning sites through a cooperative action of a doublet of defects.

[1] P. G. de Gennes, Rev. Mod. Phys. **57**, 827 (1985).
[2] L. Leger and J. F. Joanny, Rep. Prog. Phys. **55**, 431 (1992).
[3] T. Halpin-Healy and Y. C. Zhang, Phys. Rep. **254**, 215 (1994).
[4] A. L. Barabási and H. E. Stanley, *Fractal Concepts in Surface Growth* (Cambridge University Press, Cambridge, 1995).
[5] M. Kardar, G. Parisi, and Y. C. Zhang, Phys. Rev. Lett. **56**, 889 (1986).
[6] M. A. Rubio, C. A. Edwards, A. Dougherty, and J. P. Gollub, Phys. Rev. Lett. **63**, 1685 (1989); V. K. Horváth, F. Family, and T. Vicsek, J. Phys. A **24**, L25 (1991); Phys. Rev. Lett. **65**, 1388 (1990); M. A. Rubio, A. Dougherty, and J. P. Gollub, *ibid.* **65**, 1389 (1990); S. He, G. L. M. K. S. Kahanda, and P. Z. Wong, *ibid.* **69**, 3731 (1992).
[7] M. Čieplak and M. O. Robbins, Phys. Rev. Lett. **60**, 2042 (1988).
[8] M. Čieplak and M. O. Robbins, Phys. Rev. B **41**, 11 508 (1990).
[9] P. G. de Gennes, J. Phys. (Paris) **47**, 1541 (1986).
[10] S. Maslov, Phys. Rev. Lett. **74**, 562 (1995).
[11] S. Roux and A. Hansen, J. Phys. (France) I **4**, 515 (1994).
[12] S. B. Santra and I. Bose, J. Phys. A. **26**, 3669 (1993).
[13] C. W. Park and G. M. Homsy, J. Fluid Mech. **139**, 291 (1984).
[14] A. Paterson, M. Fermigier, P. Jenffer, and L. Limat, Phys. Rev. E **51**, 1291 (1995).
[15] Y. C. Zhang, J. Phys. (Paris) **51**, 2129 (1990).
[16] J. Schmittbuhl, J. P. Vilotte, and S. Roux, Phys. Rev. E **51**, 131 (1995).
[17] J. M. di Meglio, Europhys. Lett. **17**, 607 (1992); G. D. Nadkarni and S. Garoff, *ibid.* **20**, 523 (1993).
[18] J. F. Duprat, M. Fermigier, F. Goulaouic, and P. Jenffer, C. R. Acad. Sci. Paris II **314**, 879 (1992).
[19] P. Bak, C. Tang, and K. Wiesenfeld, Phys. Rev. Lett. **59**, 381 (1987); Phys. Rev. A **38**, 364 (1988).
[20] H. M. Jaeger, C. Liu, and S. R. Nagel, Phys. Rev. Lett. **62**, 40, (1989); G. A. Held, D. H. Solina, D. T. Keane, W. J. Haag, P. M. Horn, and G. Grinstein, *ibid.* **65**, 1120 (1990); M. Caponeri, S. Douady, S. Fauve, and C. Laroche, in *Mobile Particulate Systems,* edited by E. Guazzelli and L. Oger (Kluwer Academic, Dordrecht, 1995).
[21] R. Lenormand and S. Bories, C. R. Acad. Sci. Ser. B **291**, 279 (1980); D. Wilkinson and J. F. Willemsen, J. Phys. A **16**, 3365 (1983).
[22] K. J. Måløy, L. Furuberg, J. Feder, and T. Jøssang, Phys. Rev. Lett. **68**, 2161 (1992).
[23] J. M. Carlson, J. S. Langer, B. E. Shaw, and C. Tang, Phys. Rev. A **44**, 884 (1991).
[24] J. Schmittbuhl, J. P. Vilotte, and S. Roux (unpublished).
[25] D. François, A. Pineau, and A. Zaoui, *Elasticité et Plasticité* (Hermès, Paris, 1993).
[26] J. Friedel, *Dislocations* (Pergamon, Oxford, 1964).
[27] N. F. Mott and F. R. N. Nabarro, Proc. Phys. Soc. London **52**, 86 (1940).